



Synthesis of ZnO nanostructure using activated carbon for photocatalytic degradation of methyl orange from aqueous solutions

Mahda Sadat Nasrollahzadeh¹ · Mojtaba Hadavifar² · Seyedeh Sima Ghasemi² · Mansour Arab Chamjangali³

Received: 23 March 2018 / Accepted: 12 June 2018 / Published online: 20 June 2018
© The Author(s) 2018

Abstract

In this research, zinc oxide (ZnO) nanostructure was prepared by using zinc acetate (as precursor) and carboxylic derivative of activated carbon (as matrix). Activated carbon was modified by oxidation with nitric acid to get carboxylic derivative (AC-COOH). Then, zinc was loaded on the surface of modified activated carbon by an impregnation method. The ZnO nanostructure was characterized by BET, XRD and SEM that confirmed achieving of ZnO nanoparticles with a size of 21–31 nm and surface area of 17.78 m² gr⁻¹. The efficiency of the catalyst was evaluated in the photocatalytic decomposition of aqueous solution of azo dye methyl orange (MO). Major parameters such as pH, dose of catalyst, stirring effect, initial concentration of dye and solution oxygen effect were considered. Activity measurements under UV radiation showed acceptable results for the photodegradation of MO. The efficiency of catalyst prepared with non-modified activated carbon for the photodegradation of MO was also evaluated. The results confirmed that ZnO prepared using carboxylic derivative of activated carbon as matrix had better photocatalytic activity than ZnO prepared by non-modified carbon matrix.

Keywords Zinc oxide · Activated carbon · Photodegradation · Methyl orange

Introduction

Wastewaters containing reactive dyes discharged from various industries often cause many environmental problems (Doulati Ardejani et al. 2005). These wastewaters cause many damage to the ecological system of the receiving surface water bodies (Georgiou et al. 2002; Tsui et al. 2003). Considerable efforts have been done by many researchers to find appropriate treatment methods in order to remove pollutants and impurities from wastewaters emanated from different industries (Ramakrishna and Viraraghavan 1998; Hachem et al. 2001; Annadurai et al. 2002; Georgiou et al. 2002; Gökmen and Serpen 2002; Mohan et al. 2002; Tsui

et al. 2003). Many chemical and physical methods of dyes removal including membranes (Wu et al. 1998), adsorption techniques (Annadurai et al. 2002; Mohan et al. 2002) and photocatalytic degradation (Hachem et al. 2001) have been used from past to present. Recently, photocatalytic degradation as one of advanced oxidation processes (AOPs) has been used for removal of dyes from wastewaters by many researches (Daneshvar et al. 2007). The photocatalytic reaction occurs by light and a substrate (catalysis) without any change in the substrate that under this situation the reaction rates can be increased (Horikoshi et al. 2002). Because of low fraction energy between capacity and conduction bands, semiconductors play a catalysis role in suitable conditions (Parida et al. 2006). In photocatalytic process, an energy equal different of two level be needed. Adsorption of this energy causing to move electrons leading to formation of hole (h⁺) and electron (e⁻) pair. Electrons can participate at the reduction in electron acceptor species and oxidation of electron donor species (Khataee et al. 2011).

Many of materials such as TiO₂, ZnO, ZrO₂, CdS, MoS₂ and WO₃ as photocatalysis are used to degradation of pollutants (Pirkanniemi and Sillanpää 2002; Heidari et al. 2009; Ghasemi et al. 2016a, b). Among these materials, TiO₂ is

✉ Mojtaba Hadavifar
mhadavifar@yahoo.com; m.hadavifar@hsu.ac.ir

¹ Department of Medicinal Chemistry, Pharmacy Faculty, Mashhad University of Medical Sciences, Mashhad, Iran

² Department of Environmental Sciences, Hakim Sabzevari University, P.O. Box 397, Sabzevar 9617976487, Iran

³ College of Chemistry, Shahrood University of Technology, Shahrood, Iran

common photocatalysis and has had a maximum applied so far. TiO_2 has advantages such as compatibility with environment and non-toxicity, chemical stability and capability of recovery and reusing. Nonetheless, TiO_2 has defects such as high cost and adsorption band at ultraviolet area. Hence, recently ZnO as a good replacement for TiO_2 at the photocatalytic process is noteworthy (Linsebigler et al. 1995).

Zinc oxide is one of richest structures that have many advantages. So ZnO has many applications at the different studies of researches (Ni et al. 2005; Chen et al. 2007; Salavati-Niasari et al. 2009). Many methods have been used for synthesizing the ZnO such as soft chemical method (Vayssieres 2003), sol–gel process (Zhang et al. 2003), vapor phase growth (Sun et al. 2004), vapor–liquid–solid process (Gao and Wang 2004), electrophoretic deposition (Liu et al. 2003; Illy et al. 2005), thermal evaporation (Umar and Hahn 2006), homogeneous precipitation (Liu et al. 2007), chemical vapor deposition (Okazaki et al. 2011), chemical bath deposition (Yuliarto et al. 2015), etc. At the mentioned researches, only in some cases ZnO nanoparticles were synthesized by activated carbon bed and with the auxiliary matrix method such as those applied by Park et al. (Park et al. 2008). Also in none photocatalytic activity synthesis of ZnO by auxiliary matrix method for degradation of organic dyes had not been studied yet and also in all of those methods not seen any modification onto activated carbon before using as bed to producing the ZnO. Therefore, in this research for first time, the ZnO was synthesized by modified activated carbon (with carboxylic functional groups) and also photocatalytic activity of obtained ZnO has been used for degradation of methyl orange azo dye.

Materials and methods

Reagents

All chemicals such as zinc acetate ($\text{Zn}(\text{CH}_3\text{CO}_2)_2 \cdot 2\text{H}_2\text{O}$), activated carbon (AC), sodium hydroxide (NaOH), acid hydrochloride (HCl), nitric acid (HNO_3) and methyl orange ($\text{C}_{14}\text{H}_{14}\text{N}_3\text{O}_3\text{SNa}$) with the highest purity are purchased from Merck, Darmstadt, Germany. The stock solution ($100 \mu\text{g mL}^{-1}$) of methyl orange was prepared by dissolving 0.010 g of the methyl orange in 100 mL double-distilled water. All working solutions with desired concentration were prepared by diluting the stock solution with distilled water.

Experimental and equipment

UV–Vis spectra for record of a Rayleigh UV–visible spectrophotometer model UV-2601 equipped with a pair of 1.0 cm quartz cells were utilized. A Metrohm pH-meter (model 744) was used in order to adjust the pH of the working solution

at desirable values. The shape and surface morphology of samples were investigated by field emission scanning electron microscope (FESEM, Hitachi S4160, Japan). The X-ray diffraction patterns (XRD) were recorded using BRUKER, model B8 ADVANCE. Inductively coupled plasma (ICP) model (VISTA-PRO) was used for measuring zinc in the samples. Infrared (IR) spectrum of samples was recorded using spectrophotometer (IR-470 Shimadzu). Experiments of degradation and photocatalytic bleaching methyl orange pigment were performed in a photoreactor setup designed in the laboratory of analytical chemistry. The photoreactor used for the experiments was designed and built in dimensions of $75 \times 60 \times 90$ cm in the laboratory scale for photocatalytic reactions. A magnetic stirrer for agitating the reaction solution was placed inside the reactor. UV radiation was supplied using an adjustable F8T5 UV-B, 302-nm fluorescent black tube (made in Japan), ($5300 \mu\text{W cm}^{-2}$ UV-B; $1150 \mu\text{W cm}^{-2}$ UV-A and $3.9 \mu\text{W cm}^{-2}$ UV-C). The distance between the UV lamp and reaction vessel surface was fixed at 50 mm. Double-walled Pyrex container was used as a reactor and cooled by water circulator when required. Two input and output valves contrived on the reactor vessel to purge oxygen and nitrogen gas as required.

Synthesizing of ZnO nanoparticles using modified carbon particles

Surface modification of activated carbon

The functionalizing of activated carbon particles was conducted according to Chang et al. (Li et al. 2009) method to entail the carboxylic functional groups onto activated carbon surface. Activated carbon powder was first purified with 10% (v/v) hydrochloric acid solution for 24 h to remove the metal ions and other impurities. Then, 10 g of purified activated carbon was suspended in 300 mL of 32.5% (v/v) nitric acid of solution under stirring and heating for 5 h at 60°C . The mixture was filtered and washed with deionized water to neutral and was dried under vacuum at 80°C for 8 h. The product was carboxylic derivative of activated carbon (AC–COOH).

Synthesizing of ZnO nanoparticles

2.0 grams of carboxylated activated carbon (AC–COOH) with 100 ml of zinc acetate solution (as a precursor for the synthesis of zinc oxide nanoparticles) was stirred for 12 h with various concentrations. The solution was filtered and dried for 18 h in an oven at 80°C and then was calcined in electric furnace at 500°C for 4 h. In order to study the effect of zinc acetate precursor concentration on characterization of ZnO (percentage, particle size, photocatalytic properties, etc.), various concentrations of zinc acetate were examined

to prepare ZnO nanoparticles by above-mentioned method. For this purpose, solutions with concentrations of 0.01, 0.02 and 0.09 M of zinc acetate were used for the synthesis of ZnO nanoparticles. The synthesized samples of ZnO were labeled with (a), (b) and (c) for different concentrations of 0.01, 0.02 and 0.09 M of zinc acetate, respectively. In order to confirm the formation of the ZnO nanoparticle, XRD spectra were recorded for three samples. The crystal size of three samples was estimated using width tapes XRD pattern and Scherrer's Eq. (1) (Scherrer 1918; Skoog and West 1980):

$$D = K \left(\frac{\lambda}{\beta \cos \theta} \right) \quad (1)$$

where D is the crystalline particle size in terms of nm, K (0.89) is a coefficient, λ is wavelength of the X-ray in nm, β is the experimental full width at half-maximum (FWHM) in radians, and θ is diffraction angle in terms of degrees.

Synthesizing of ZnO nanoparticles using unmodified carbon particles

In order to investigate the surface modification of activated carbon in the synthesis of ZnO, 2.0 g activated carbon was placed in 200 ml HCl solution of 10% (v/v) in order to remove impurities for 24 h. Thereafter, concentration of 0.09 M of zinc acetate solution was added to product for 12 h and then filtered the resulting mixture. Final product was dried for 18 h at 80 °C and then was calcined in electric oven at 500 °C for 4 h. XRD spectra were recorded for sample synthesized with unmodified activated carbon to evaluate crystal size of the sample using Scherrer's equation.

Photocatalytic experiments degradation of methyl orange

First, 100 ml of methyl orange solution with a concentration of 10 mg L⁻¹ and pH 6 was prepared and transferred into a 250-mL beaker. Then, 20 mg of ZnO photocatalyst was added to the solution. To perform adsorption of methyl orange on ZnO nanoparticles, the solution was mixed using a magnetic stirrer in dark media for 30 min. After making sure of the adsorption equilibrium, 0.2 ml of solution was transferred into a test tube and was centrifuged at 3000 rpm for 5 min for deposition particulate photocatalyst. The adsorption spectrum of solution was recorded by spectrophotometer in the region of 200–600 nm. After recording the absorption spectrum, the mixture was placed inside a photoreactor and UV lamp was lit. Ten samples were taken with intervals of 20 min after UV radiation, and their absorption spectrum was recorded. To record the adsorption spectrum of control solution the same way acted without using any photocatalyst in the solution.

Batch adsorption experiments

Batch experiments were conducted in order to obtain the optimal conditions for bleaching and degradation of methyl orange in the presence of the ZnO photocatalysts. The impact of influential variables such as pH, photocatalyst dose, MO (methyl orange) concentration, stirring the solution and oxygen of the solution was well investigated. To optimize variables affecting on reaction, optimizing one variable at a time was used. In this method, the experiments were conducted in batch condition with placing of 100 mL dye solution (10 mg L⁻¹) into a 250-mL beaker. Suspensions were mixed by magnetic stirrer in dark condition for 30 min and centrifuged at 3000 rpm for 5 min. The clear supernatant was analyzed by UV–Vis spectrophotometer. The rate bleaching and dye degradation was calculated by using Eq. (2) (Nekouei et al. 2016a).

$$R = \frac{C_0 - C_t}{C_0} \times 100 \quad (2)$$

In this equation, R (%) is dye removal efficiency, C_0 is the initial concentration of the dye (mg L⁻¹), and C_t is the concentration of dye at time t after adsorption (mg L⁻¹).

Results and discussion

Characterization of nanoparticles

XRD analysis

Figure 1 shows XRD spectra recorded for three prepared ZnO samples in order to confirm the appropriate formation of ZnO nanoparticles. According to the Figures, the formation of hexagonal crystals of zinc oxide in the sample has been confirmed. For comparison, the parameters of XRD patterns for three prepared samples and the standard sample (Yuliarto et al. 2015) are summarized in Table 1. According to the XRD spectra shown in Fig. 1 and data of Table 1, it is observed that increasing zinc acetate concentration resulted in increasing of ZnO peak intensities and also reduced spectral noise density. This evidence can be due to the enhanced formation of ZnO nanostructures with increasing zinc acetate concentration. In XRD spectra, intensity of peak 005 is related to impurities of carbon (Liu et al. 2007) that reduced with increase in zinc acetate concentration. Figure 2 shows XRD spectra recorded for the synthesized sample with unmodified carbon. Also from Table 1 and comparison of XRD data of synthesized sample (unmodified carbon and the standard sample), the formation of hexagonal ZnO has been approved. Table 2 shows the crystal size of three samples synthesized with modified and unmodified carbon.

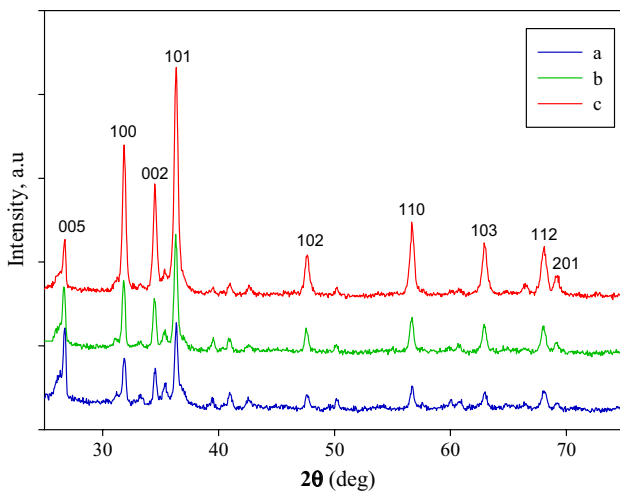


Fig. 1 XRD spectra of synthesized ZnO nanoparticles with different concentration of 0.01 (a), 0.02 (b) and 0.09 M (c) of zinc acetate

ICP, BET and SEM analysis

ICP analysis was done in order to calculate the ZnO percent in samples. ICP analysis showed that the ZnO amount in samples a, b and c was 9.94, 10.74 and 31.81%, respectively. These results indicate that increasing zinc acetate concentration concludes an enhancement in ZnO percent of the samples. ICP analysis for unmodified carbon showed that ZnO percent was 19.8%, indicating that without surface modification of activated carbon, composed ZnO percent is reduced. BET analysis was conducted to determine the specific surface area of synthesized ZnO nanoparticles (only for sample c). Results of the BET analysis showed specific surface area of 7.78 m² g⁻¹, total pore volume 0.1 cm³ g⁻¹ and average pore diameter 51.6 nm that its specific surface area is more than specific surface area of commercial ZnO (4.49 m² g⁻¹) (Lee et al. 2009). This increased level is due to the presence of activated carbon in the synthesized ZnO. Characterization of surface morphological and textural of the activated carbon, ZnO and AC–ZnO catalysts are important parameters and might increase efficacy of

Table 1 Comparing of XRD samples (a), (b) and (c) and sample synthesized using unmodified carbon with standard sample

Standard sample (card No: 39-1451)	Samples									
	(a)			(b)			(c)			Sample synthesized using unmodified carbon
hkl	d (Å)	I/I ₀	d (Å)	I/I ₀	d (Å)	I/I ₀	d (Å)	I/I ₀	d (Å)	I/I ₀
100	2.81	57	2.80	67	2.81	66	2.80	68	2.74	31
002	2.60	44	2.59	85	2.59	54	2.59	52	2.51	90
101	2.47	100	2.46	100	2.47	100	2.47	100	2.31	100
110	1.62	32	1.62	41	1.62	39	1.62	36	1.50	32

d distance between plates in terms of angstrom, I peak intensity, I₀ maximum intensity to the planes 100 and 002, 101 and 110

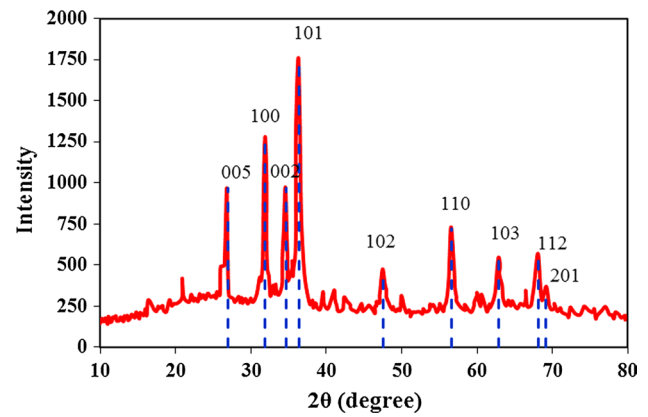


Fig. 2 XRD spectra sample was synthesized using an unmodified carbon with concentration of 0.09 M of zinc acetate

Table 2 Estimated particles size from Scherrer's equation

Planes	Sample size (nm)			
	(a)	(b)	(c)	Sample synthesized using an unmodified carbon
101	25	24	21	23.50
100	26	27	23	35.66
002	32	26	24	24.34

the photocatalytic activity (Sobana et al. 2008). To study the morphology feature of synthesized of ZnO nanoparticles, scanning electron microscopy (SEM) was recorded for samples a, b and c demonstrated in Fig. 3. It can be seen that with increase in zinc acetate concentration the pores of activated carbon are occupied by ZnO particles obtaining a homogeneous coverage and many of the activated carbons were covered by ZnO particles. Although the large holes of activated carbon have been occupied by ZnO particles, blocking the porosity of the carbon surface, the sample c still shows a porous character with a relatively large pore volume and surface area (Muthirulan et al. 2013).

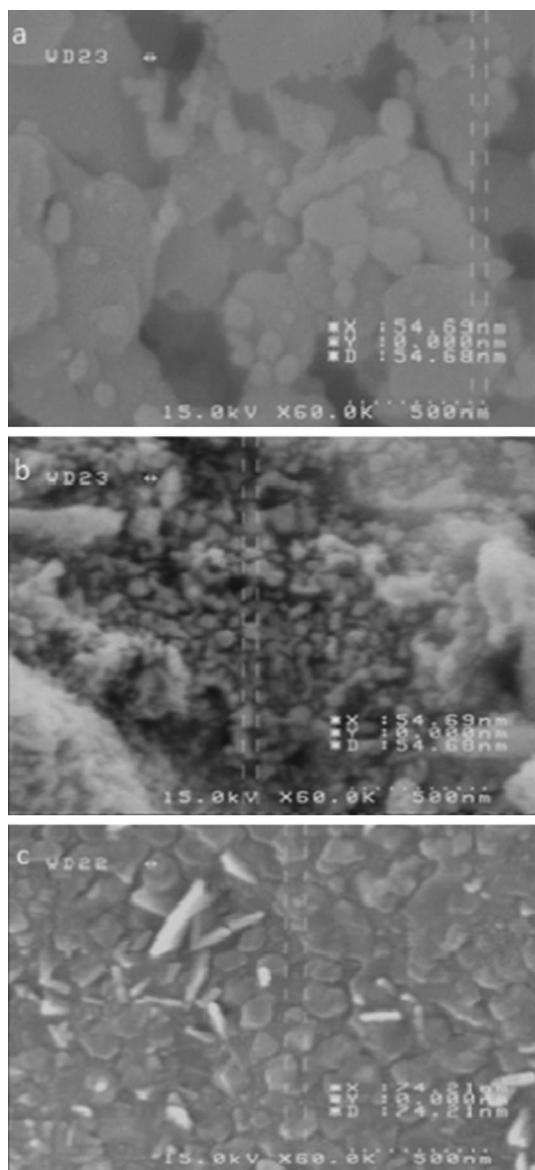


Fig. 3 Scanning electron micrograph image from samples a, b and c

UV-Vis spectroscopic analysis

In the adsorption spectrum of methyl orange, it can observe two adsorption bands at wavelengths of 464 and 272 nm. Decrease in the absorption band at 464 nm is due to azo bond broken down resulting a bleaching process, while decrease in the absorption in the region 272 nm is due to degradation of phenyl rings and complete mineralization of methyl orange. As can be seen in Fig. 4, in the absence of ZnO photocatalyst, decolorization rate is very low and does not occur complete degradation or mineralization. Whereas is shown in Fig. 5, in the presence of ZnO nanoparticles catalyst, complete bleaching and degradation occurs. For further investigation, according to Fig. 6, the absorption

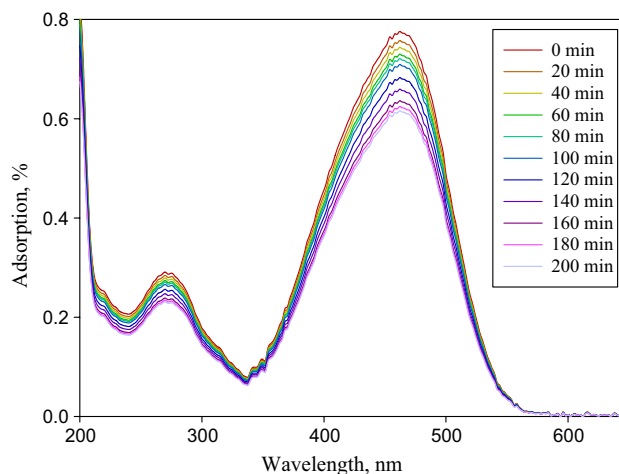


Fig. 4 Adsorption spectrum of reaction system in the absence of ZnO photocatalyst, methyl orange 10 mg L⁻¹ and pH 6

trend with time was performed at the wavelengths of 464 and 272 nm in three conditions of darkness, UV radiation and finally UV radiation in presence of the catalyst. The figure indicates that complete bleaching rate and degradation of methyl orange occur due to photochemical reaction in the presence of ZnO catalyst in time 200 min, whereas in the absence of photocatalyst degradation and bleaching processes were almost negligible. Data analysis showed that the adsorption process of methyl orange on the catalyst surface stabled in 20 min after stirring the mixture of dye and catalyst in the condition of darkness and no mere degradation occurs. So in all investigations to ensure reaching adsorption equilibrium, mixture of dye and catalyst was stirred in the darkness condition for 30 min.

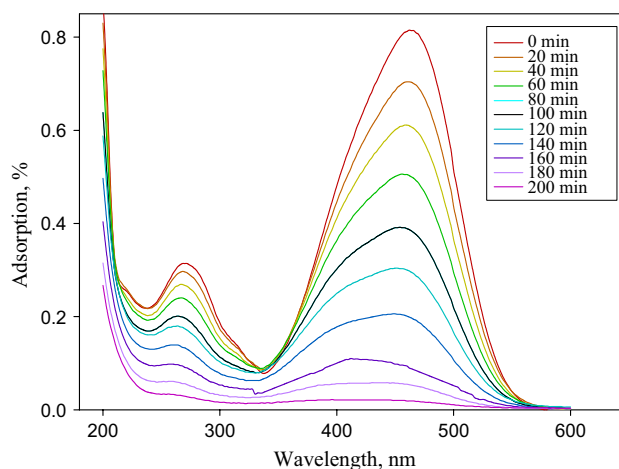


Fig. 5 Adsorption spectrum of reaction system at presence of ZnO photocatalyst for 200 mg L⁻¹ photocatalyst, methyl orange 10 mg L⁻¹ and pH 6

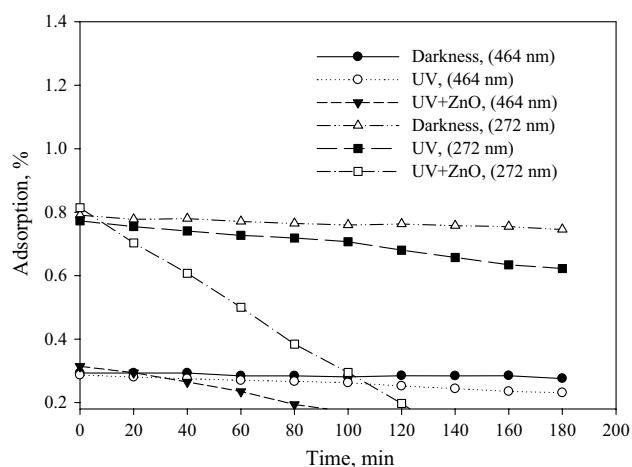


Fig. 6 Changes in absorption with time at wavelengths of 272 and 464 nm, conditions 200 mg L^{-1} of photocatalyst, methyl orange 10 mg L^{-1} and pH 6

Effect of pH

The pH has a crucial impact on the adsorption capacity of adsorbent and removal efficiency via changing the adsorption chemistry of adsorbent–adsorbate (Nekouei et al. 2016b). The pH-related experiments were carried out in the various pH values (4–10) with 20 mg of photocatalyst into 100 mL of the dye solution (10 mg L^{-1}) at the optimum contact time. The adjustment of the solution pH was conducted by 0.1 M HCl and 0.1 M NaOH solution. The influence of solution pH on the rate bleaching and degradation of MO by AC–ZnO is shown in Fig. 7. It is evident that the maximum rate bleaching and dye degradation of MO is observed at pH 6. So pH 6 was selected for further studies. Such a process in removal dependency to the pH can be attributed to electrostatic attraction variations between the ZnO surface and dye MO. This optimum electrostatic attraction leads to better adsorption of the pollutant onto the adsorbent particles in comparison with the acidic conditions (in which the driving force is stronger) (Noorimotlagh et al. 2016). Surface charge for ZnO at low pH 9 is positive (Daneshvar et al. 2007). Therefore, anions adsorption in an aqueous environment on ZnO at low pH 9 is more. On the other hand, the given pKa for methyl orange is 3.8 ± 0.02 (Štastná et al. 2005). Therefore, at the pH above the pKa, anionic form of methyl orange concentration is more than cationic form. With increasing the solution pH to 6, adsorption of methyl orange onto ZnO was increased. Decrease in the rate bleaching and dye degradation was observed at higher pH value above 6 because of this fact that the oxidation potential of hydroxyl radical decreases with increasing of pH solution (Lucas and Peres 2006). Additionally, the increased concentration of OH^- in the solution concludes a competition between OH^- ions and anionic form of methyl orange (Saini

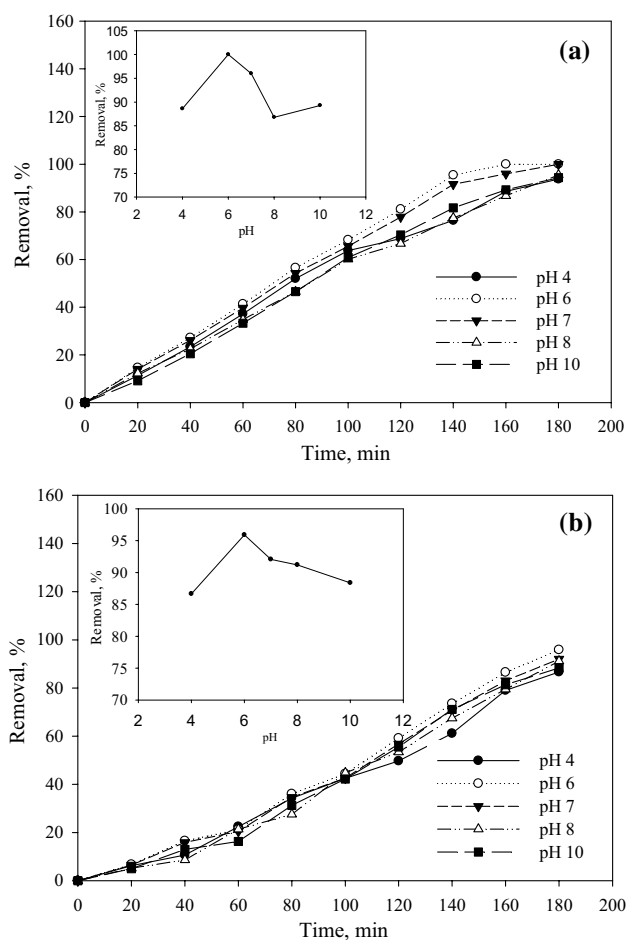


Fig. 7 Effect of pH on the rate bleaching (a) and dye degradation (b) of MO for 200 mg L^{-1} photocatalyst, methyl orange 10 mg L^{-1}

et al. 2017) that decreases adsorption of methyl orange onto ZnO.

Effect of photocatalysts dose

In order to examine the effect of photocatalyst dose on the bleaching and degradation of MO, different amount of catalyst from 100 to 500 mg L^{-1} were added to solution at a reaction time of 180 min, pH of 6 and initial MO concentration of 10 mg L^{-1} . The results of these analyses are shown in Fig. 8. The results demonstrated that the bleaching and degradation was increased with increasing the amount of catalyst to 200 mg L^{-1} , showing no significant change in bleaching and degradation with increasing the amount of catalyst to 400 mg L^{-1} , but the bleaching and degradation was decreased with increasing the amount of catalyst to 500 mg L^{-1} . This is due to the availability of surface active sites that increased with increasing the amount of catalyst. Consequently, increased production of hydroxyl radicals occurs causing increased photocatalytic activity

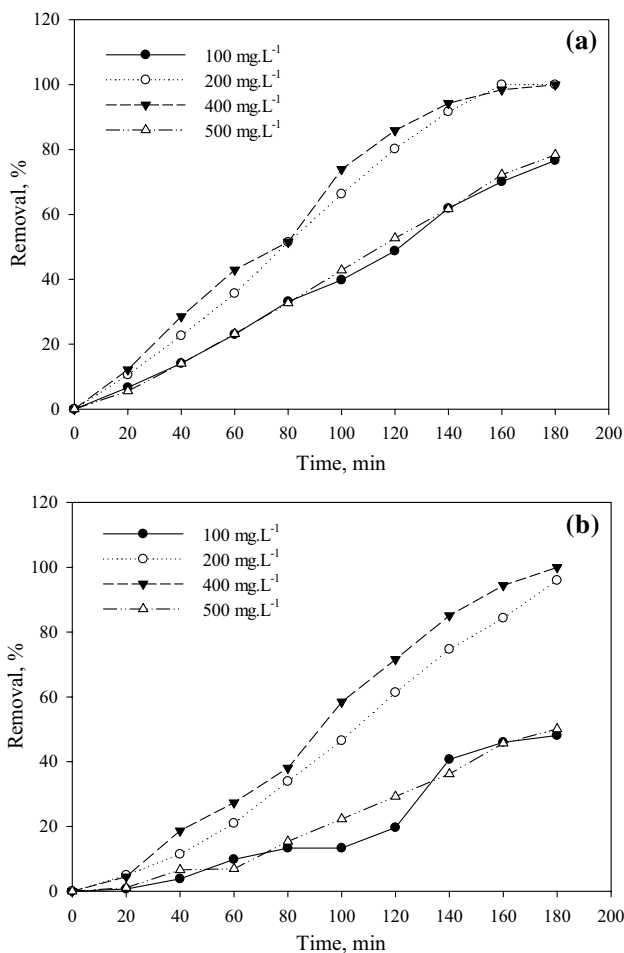


Fig. 8 Effect of catalyst amount on the rate bleaching (a) and dye degradation (b) of MO. Methyl orange of 10 mg L⁻¹, pH 6 and time 180 min

of ZnO. With excessive increase catalyst milky solution prevents penetrating of UV light onto the catalyst surface. Consequently, these phenomena can decrease production of hydroxyl radicals, decreasing efficiency dye damage and discoloration of solution (Mills et al. 1993; Daneshvar et al. 2007). Therefore, dose of 200 mg L⁻¹ photocatalyst was selected for further studies.

Effect of MO concentration

To determine the effect of initial MO concentration on the efficiency of the process, various MO concentrations (5–20 mg L⁻¹) at a reaction time of 180 min and an initial pH of 6 were examined. The results of these analyses are shown in Fig. 9. The results demonstrated that the bleaching and degradation was decreased with increasing the initial dye concentration. This may be due to the decrease in the availability of surface active sites. Consequently, production of hydroxyl radicals decreases and this can decrease

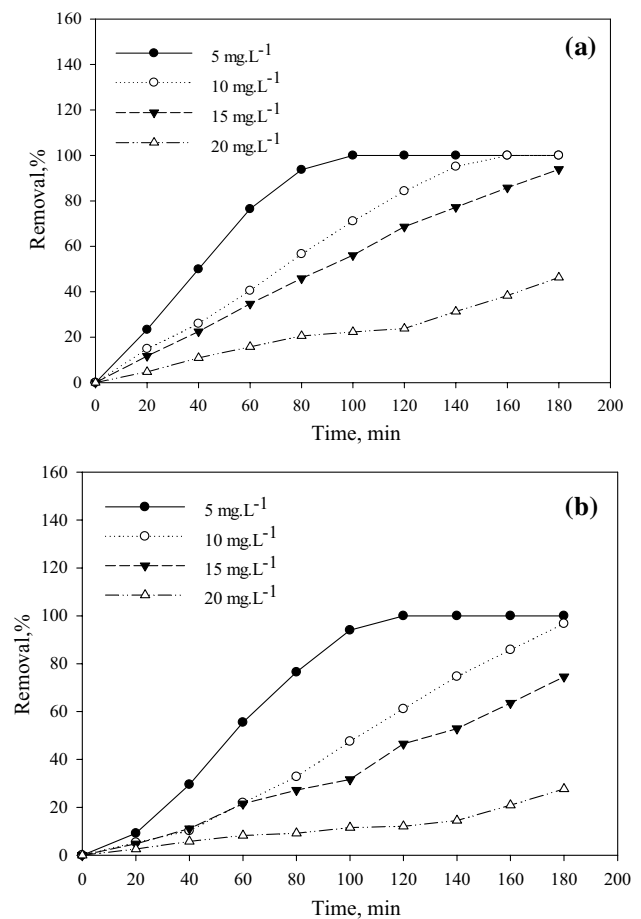


Fig. 9 Effect of initial concentration of methyl orange on the rate bleaching (a) and dye degradation (b) for pH 6, 200 mg L⁻¹ photocatalyst

photocatalytic activity. On the other hand, the increase in dye concentration also decreases the path length of photon entering into the dye solution. At high dye concentration, the dye molecules may absorb a significant amount of solar light rather than the catalyst and this may also reduce the catalytic efficiency (Rao et al. 2009; Sobana et al. 2013). Therefore, MO concentration of 10 mg L⁻¹ was selected for further study.

Effect of stirring the solution

In order to examine the effect of stirring the solution on the bleaching and degradation of MO, some experiments were done at a reaction time of 180 min, pH of 6, initial MO concentration of 10 mg L⁻¹ and amount of catalyst 200 mg L⁻¹. The results of these analyses are shown in Fig. 10. The results demonstrate that the bleaching and degradation was increased under stirring of the solution. Firstly, agitation makes a turbulent in the solution that increases solving of oxygen into the solution. Soluble oxygen plays an important

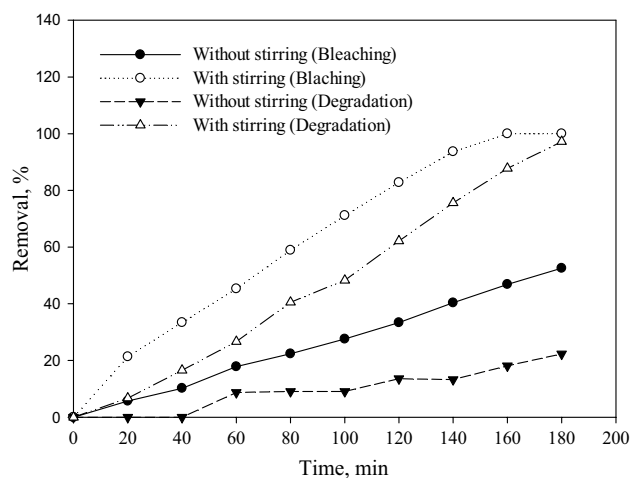


Fig. 10 Effect of stirring the solution on the rate bleaching and dye degradation of MO. pH 6, 20 mg L⁻¹ photocatalyst, 10 mg L⁻¹ MO concentration

role in production of hydroxyl radicals. Secondly, stirring the solution leads to decrease in equilibrium time by increase in rate of MO transfer and diffusion to the adsorbent surface (Ghaedi et al. 2014).

Effect of oxygen the solution

In order to examine the effect of oxygen, the solution on the bleaching and degradation of MO studies was conducted in the air atmosphere and nitrogen atmosphere in condition of initial pH 6, initial MO concentration of 10 mg L⁻¹, amount of catalyst 200 mg L⁻¹ and passing time of nitrogen gas into solution 3 min. The results of these analyses are shown in Fig. 11. The results demonstrate that the bleaching and degradation efficiency in the presence of oxygen was much higher compared to the absence of oxygen in the solution. This is due to the trapping electrons by oxygen in conduction bands of the semiconductor (photocatalyst) producing radicals and oxidants species such as HO₂, H₂O₂ and O₂ (Anne 1993) that these radicals and oxidant agents can increase efficiency of bleaching and degradation.

Effect of precursor concentration on the photocatalytic activity

Deposition of zinc oxide onto the surface of photocatalyst investigated by three different precursor concentrations of 0.01, 0.02 and 0.09 M of zinc acetate and obtained products was applied for the reaction of methyl orange degradation and bleaching. ICP analysis of zinc oxide for three samples a, b and c revealed 9.94, 10.74 and 31.81% of ZnO for each, respectively. Figure 12 demonstrates the bleaching and degradation of MO. As figure shows,

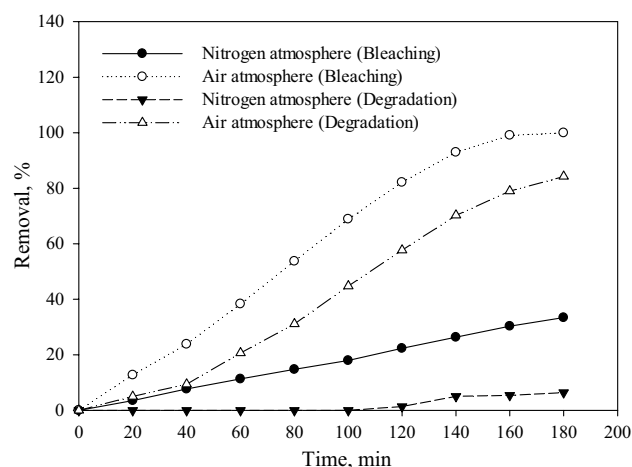


Fig. 11 Effect of oxygen on the rate bleaching and dye degradation of MO. pH 6, 200 mg L⁻¹ photocatalyst, 10 mg L⁻¹ MO concentration

increased precursor concentration concluded an enhanced bleaching and degradation values. According to the results of Park et al., it was inferred that the growth of ZnO nanostructures as a function of the amount of zinc doped on the matrix, caused by an effect of CO produced from the decomposition of acetate group by oxidation in the case that zinc acetate was used as a precursor.

Effect of modification of modified activated carbon on the photocatalytic activity of ZnO

In the present study, synthesis of photocatalyst has been done using modified activated carbon. The effect of modified and unmodified activated carbon on the bleaching and

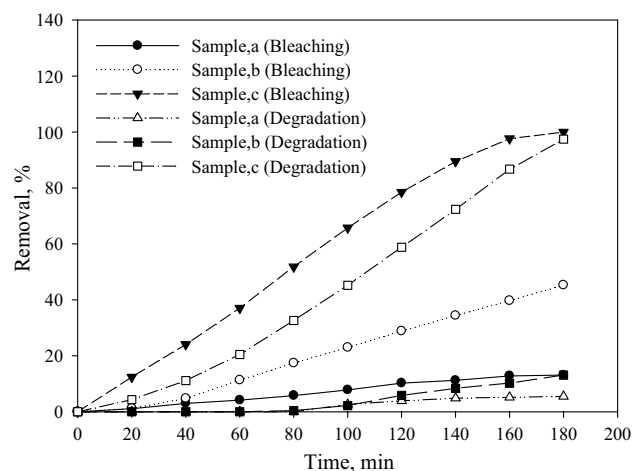


Fig. 12 Effect of precursor concentration on the rate bleaching and dye degradation of MO. pH 6, 200 mg L⁻¹ photocatalyst, 10 mg L⁻¹ MO concentration

degradation of MO is shown in Fig. 13. The results demonstrate that the bleaching and degradation efficiency in the presence of zinc oxide synthesized with modified activated carbon was much higher than unmodified one. Carboxylic acid on the surface of activated carbon is very effective in adsorption of Zn²⁺ ion from aqueous solutions and its conversion into zinc oxide. As mentioned earlier, ICP analysis results indicated that ZnO percent in synthesized sample with unmodified activated carbon was 19.8% that this resulted a decreased bleaching and degradation efficiency.

Effect of calcination temperature on the activity of photocatalysts

Three calcination temperatures of 450, 500 and 550 °C were applied in order to investigate the temperature effects of the calcination process on the activity of ZnO photocatalysts. The activity of photocatalysts of these samples in the degradation and bleaching of MO is shown in Fig. 14. The results demonstrate that the photocatalytic activity increased with increase in calcination temperature to 500 °C and after that remained almost stable. Low photocatalytic activity obtained in temperature 450 °C may be due to this fact that not enough temperature has been prepared to complete burning of carbon substrate, so the amount of ZnO in a certain amount of catalyst increased with increase in calcination temperature to 500 °C.

Effect interference of ions

Ions solution in the effluents may compete with dye molecules for active sites on the surface of the catalyst. So it is possible to deactivate the photocatalyst and decreased rate degradation of the target dye. The main reasons for the

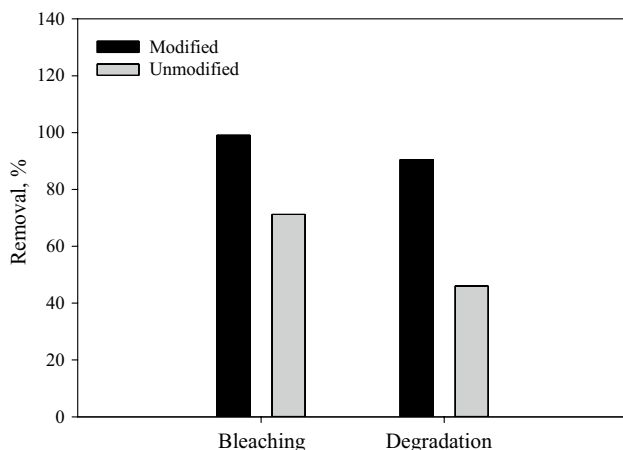


Fig. 13 Effect of surface modification of activated carbon on the rate bleaching and dye degradation of MO. pH 6, 20 mg L⁻¹ photocatalyst, methyl orange 10 mg L⁻¹, time 160 min

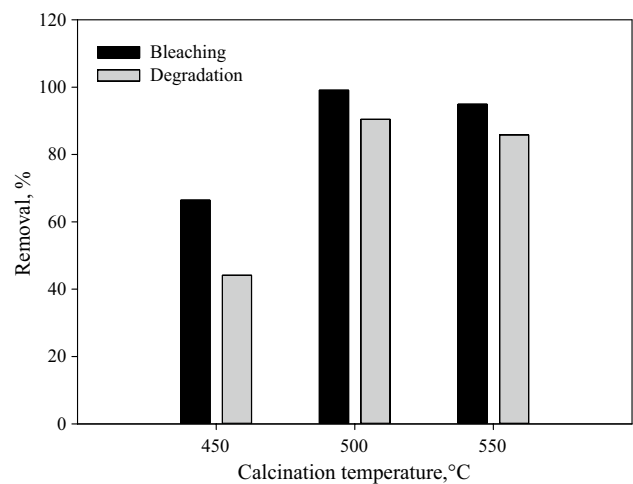


Fig. 14 Effect of calcination temperature on the rate bleaching and dye degradation of MO. pH 6, 20 mg L⁻¹ photocatalyst, methyl orange 10 mg L⁻¹, time 160 min

possible reduction in the rate degradation can be considered high activity and non-selective of •OH radical that reacted with nontarget compounds in matrix (Rauf and Ashraf 2009). The effect of some ions on the bleaching and degradation of MO in the presence of ZnO catalyst was investigated. In these experiments, rate bleaching and degradation of MO in the presence of the photocatalyst and in the absence of any other ions was measured in the optimum conditions for five successive times. Then, the percent degradation and bleaching of MO was measured in the presence of interfering ions concentrations of 1000 (mg L⁻¹). If the presence of interfering ions causing the shift of ± 5% in the average percent of bleaching or degradation, it can be said that no interference occurred. The results of these analyses are shown in Table 3. The results demonstrated that the presence of ions HCO₃⁻, SO₄²⁻ and NO₃⁻ did not interfere in the degradation and bleaching of MO. The high concentration of ions Cl⁻ decreases degradation efficiency due to its hydroxyl radical scavenging effect which occurs as follows (Habibi and Talebian 2007):



Table 3 The results influence the interference of common ions and permissible limits

Interfering ions	Permissible ion concentration (mg L ⁻¹)	
	Degradation	Bleaching
HCO ₃ ⁻ , SO ₄ ²⁻ , NO ₃ ⁻	1000	1000
Cl ⁻	500	800
Mg ²⁺	50	100



The presence of Mg^{2+} ions in solution also causes a decrease in degradation efficiency because these ions can react with MO and prevent from exposure of day onto the surface of the catalyst.

Effect of photocatalytic efficiency in real environment

In previous experiments, permissible limits of common ions interference were determined by adding these ions to the testing environment (distilled water). But significant point is that all ions are present together in the actual environment. Therefore, it is necessary that photocatalyst bleaching and degradation efficiency of MO be tested. Real environment prepared by 100 ml of tap water contains MO concentration of 10 mg L^{-1} , initial pH of 6 and amount of catalyst 200 mg L^{-1} . The results of these analyses are shown in Fig. 15. The results demonstrate that the efficiency of photocatalyst in the presence of common ions with various concentrations and other impurities was very good.

Effect of photocatalysts recovery and reuse

Recovery and reuse of photocatalyst is important from economic aspects. So photocatalyst efficiency during the successive recovery seems to be necessary. For this purpose, the

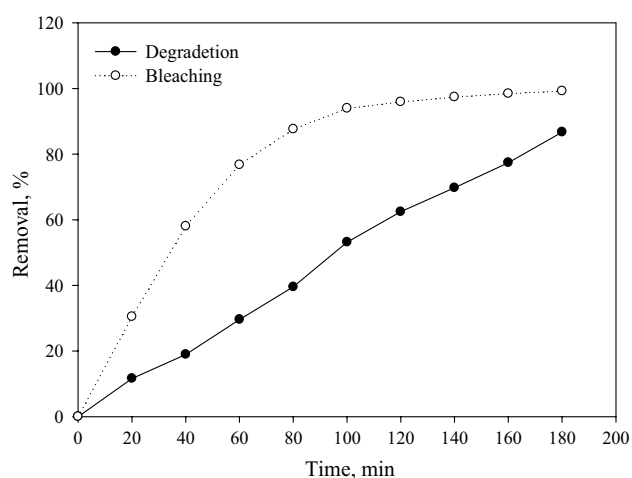


Fig. 15 Effect of photocatalytic efficiency in real environment (tap water) on the rate bleaching and dye degradation of MO. pH 6, 200 mg L^{-1} photocatalyst, 100 mL of tap water containing methyl orange 10 mg L^{-1}

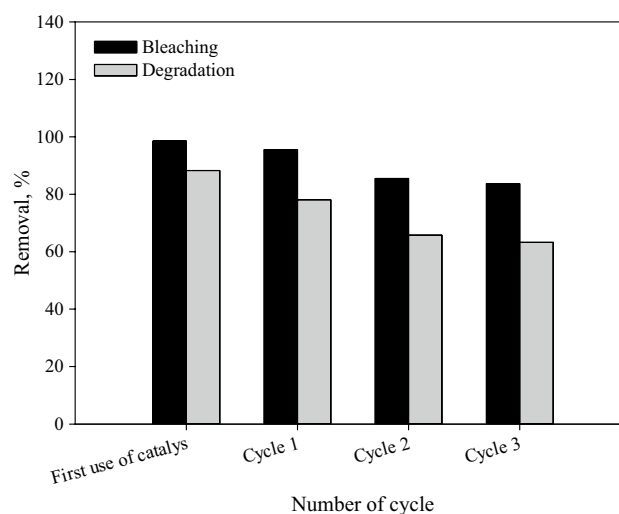


Fig. 16 Effect the number of cycles photocatalyst recovery on the rate bleaching and dye degradation of MO. pH 6, 200 mg L^{-1} photocatalyst, methyl orange 10 mg L^{-1} , time 160 min

photocatalyst used in degradation process of methyl orange was collected by centrifugation and then was washed with ethanol and distilled water. The product was dried at room temperature and then reused in degradation reaction of methyl orange. The results after the three times recovery and reuse as shown in Fig. 16 concluded a decrease in recovered catalyst efficiency. Degradation process affected more than bleaching process using recovered catalyst.

Conclusion

In the present work, dye degradation process using ZnO as a photocatalyst was investigated in degradation of methyl orange from aqueous solutions. The findings revealed that the MO dye was successfully degraded by the AC-ZnO system. The rate of degradation was high in the presence of ZnO, but lower degradation was observed in the absence of ZnO. Optimum conditions for dye degradation were determined in pH of 6, 200 mg L^{-1} of photocatalyst, 10 mg L^{-1} concentration of MO and stirring dye solution in air atmosphere. The results also showed that synthesized photocatalyst in the real environment had very good efficiency and also recovery and reuse of photocatalyst adversely caused a decrease in degradation and bleaching process. The present study provided a new efficient and low-cost adsorbent with high potential in the treatment of dye-contaminated wastewater.

Acknowledgements The authors appreciate the sponsorship of the Ministry of Science, Research and Technology of Iran, financial

supports of the Hakim Sabzevari University, Shahrood University of Technology, Iran Nanotechnology Initiative Council.

Open Access This article is distributed under the terms of the Creative Commons Attribution 4.0 International License (<http://creativecommons.org/licenses/by/4.0/>), which permits unrestricted use, distribution, and reproduction in any medium, provided you give appropriate credit to the original author(s) and the source, provide a link to the Creative Commons license, and indicate if changes were made.

References

- Annadurai G, Juang R-S, Lee D-J (2002) Factorial design analysis for adsorption of dye on activated carbon beads incorporated with calcium alginate. *Adv Environ Res* 6:191–198
- Chen Y, Yu R, Shi Q et al (2007) Hydrothermal synthesis of hexagonal ZnO clusters. *Mater Lett* 61:4438–4441
- Daneshvar N, Aber S, Seyed Dorraji MS et al (2007) Photocatalytic degradation of the insecticide diazinon in the presence of prepared nanocrystalline ZnO powders under irradiation of UV-C light. *Sep Purif Technol* 58:91–98
- Doulati Ardejani F, Singh RN, Baafi EY, Shafaei SZ (2005) A numerical model to simulate groundwater and mining interactions. In: 20th world mining congress and expo, pp 673–680
- Fox MA, Dulay MT (1993) Heterogeneous photocatalysis. *Chem Rev* 93:341–357
- Gao P, Wang ZL (2004) Nanopropeller arrays of zinc oxide. *Appl Phys Lett* 84:2883–2885
- Georgiou D, Melidis P, Aivasidis A, Gimouhopoulos K (2002) Degradation of azo-reactive dyes by ultraviolet radiation in the presence of hydrogen peroxide. *Dye Pigment* 52:69–78
- Ghaedi M, Negintaji G, Marahel F (2014) Solid phase extraction and removal of brilliant green dye on zinc oxide nanoparticles loaded on activated carbon: new kinetic model and thermodynamic evaluation. *J Ind Eng Chem* 20:1444–1452
- Ghasemi Z, Younesi H, Zinatizadeh AA (2016a) Preparation, characterization and photocatalytic application of TiO₂/Fe-ZSM-5 nanocomposite for the treatment of petroleum refinery wastewater: optimization of process parameters by response surface methodology. *Chemosphere* 159:552–564
- Ghasemi Z, Younesi H, Zinatizadeh AA (2016b) Kinetics and thermodynamics of photocatalytic degradation of organic pollutants in petroleum refinery wastewater over nano-TiO₂ supported on Fe-ZSM-5. *J Taiwan Inst Chem Eng* 65:357–366
- Gökmen V, Serpen A (2002) Equilibrium and kinetic studies on the adsorption of dark colored compounds from apple juice using adsorbent resin. *J Food Eng* 53:221–227
- Habibi MH, Talebian N (2007) Photocatalytic degradation of an azo dye X6G in water: a comparative study using nanostructured indium tin oxide and titanium oxide thin films. *Dye Pigment* 73:186–194
- Hachem C, Bocquillon F, Zahraa O, Bouchy M (2001) Decolorization of textile industry wastewater by the photocatalytic degradation process. *Dye Pigment* 49:117–125
- Heidari A, Younesi H, Zinatizadeh AAL (2009) Controllable synthesis of flower-like zno nanostructure with hydrothermal method (research note). *Int J Eng B Appl* 22:283
- Horikoshi S, Watanabe N, Onishi H et al (2002) Photodecomposition of a nonylphenol polyethoxylate surfactant in a cylindrical photoreactor with TiO₂ immobilized fiberglass cloth. *Appl Catal B Environ* 37:117–129
- Illy B, Shollock BA, MacManus-Driscoll JL, Ryan MP (2005) Electrochemical growth of ZnO nanoplates. *Nanotechnology* 16:320
- Khataee AR, Kasiri MB, Alidokht L (2011) Application of response surface methodology in the optimization of photocatalytic removal of environmental pollutants using nanocatalysts. *Environ Technol* 32:1669–1684
- Lee TJ, Cho IH, Park N-K (2009) Desulfurization using ZnO nanostructure prepared by matrix assisted method. *Korean J Chem Eng* 26:582–586
- Li Z, Chang X, Zou X et al (2009) Chemically-modified activated carbon with ethylenediamine for selective solid-phase extraction and preconcentration of metal ions. *Anal Chim Acta* 632:272–277
- Linsebigler AL, Lu G, Yates JT Jr (1995) Photocatalysis on TiO₂ surfaces: principles, mechanisms, and selected results. *Chem Rev* 95:735–758
- Liu C, Zapien JA, Yao Y et al (2003) High-density, ordered ultraviolet light-emitting ZnO nanowire arrays. *Adv Mater* 15:838–841
- Liu Y, Jian-er Z, Larbot A, Persin M (2007) Preparation and characterization of nano-zinc oxide. *J Mater Process Technol* 189:379–383
- Lucas MS, Peres JA (2006) Decolorization of the azo dye Reactive Black 5 by Fenton and photo-Fenton oxidation. *Dye Pigment* 71:236–244
- Mills A, Davies RH, Worsley D (1993) Water purification by semiconductor photocatalysis. *Chem Soc Rev* 22:417–425
- Mohan D, Singh KP, Singh G, Kumar K (2002) Removal of dyes from wastewater using flyash, a low-cost adsorbent. *Ind Eng Chem Res* 41:3688–3695
- Muthirulan P, Meenakshisundaram M, Kannan N (2013) Beneficial role of ZnO photocatalyst supported with porous activated carbon for the mineralization of alizarin cyanin green dye in aqueous solution. *J Adv Res* 4:479–484
- Nekouei F, Noorizadeh H, Nekouei S et al (2016a) Removal of malachite green from aqueous solutions by cuprous iodide–cupric oxide nano-composite loaded on activated carbon as a new sorbent for solid phase extraction: isotherm, kinetics and thermodynamic studies. *J Mol Liq* 213:360–368
- Nekouei F, Noorizadeh H, Nekouei S et al (2016b) Removal of malachite green from aqueous solutions by cuprous iodide–cupric oxide nano-composite loaded on activated carbon as a new sorbent for solid phase extraction: isotherm, kinetics and thermodynamic studies. *J Mol Liq* 213:360–368
- Ni Y, Wei X, Hong J, Ye Y (2005) Hydrothermal preparation and optical properties of ZnO nanorods. *Mater Sci Eng, B* 121:42–47
- Noorimotlagh Z, Darvishi Cheshmeh Soltani R, Shams Khorramabadi G et al (2016) Performance of wastewater sludge modified with zinc oxide nanoparticles in the removal of methylene blue from aqueous solutions. *Desalin Water Treat* 57:1684–1692
- Okazaki K, Nakamura D, Higashihata M et al (2011) Lasing characteristics of an optically pumped single ZnO nanosheet. *Opt Express* 19:20389–20394
- Parida KM, Dash SS, Das DP (2006) Physico-chemical characterization and photocatalytic activity of zinc oxide prepared by various methods. *J Colloid Interface Sci* 298:787–793
- Park NK, Lee YJ, Han GB et al (2008) Synthesis of various zinc oxide nanostructures with zinc acetate and activated carbon by a matrix-assisted method. *Colloids Surf A Physicochem Eng Asp* 313–314:66–71
- Pirkanniemi K, Sillanpää M (2002) Heterogeneous water phase catalysis as an environmental application: a review. *Chemosphere* 48:1047–1060
- Ramakrishna KR, Viraraghavan T (1998) Use of slag for dye removal. *Waste Manag* 17:483–488
- Rao AN, Sivasankar B, Sadasivam V (2009) Kinetic study on the photocatalytic degradation of salicylic acid using ZnO catalyst. *J Hazard Mater* 166:1357–1361
- Rauf MA, Ashraf SS (2009) Fundamental principles and application of heterogeneous photocatalytic degradation of dyes in solution. *Chem Eng J* 151:10–18

- Saini J, Garg VK, Gupta RK, Kataria N (2017) Journal of Environmental Chemical Engineering Removal of Orange G and Rhodamine B dyes from aqueous system using hydrothermally synthesized zinc oxide loaded activated carbon. *Biochem Pharmacol* 5:884–892
- Salavati-Niasari M, Mir N, Davar F (2009) ZnO nanotriangles: synthesis, characterization and optical properties. *J Alloys Compd* 476:908–912
- Scherrer P (1918) Bestimmung der Größe und der inneren Struktur von Kolloidteilchen mittels Röntgenstrahlen *Nachrichten von der Gesellschaft der Wissenschaften zu Göttingen, Mathematisch-Physikalische Klasse*, 2, 98–100. Cerca con Google 98–100
- Skoog DA, West DM (1980) Principles of instrumental analysis. Saunders College Philadelphia
- Sobana N, Muruganandam M, Swaminathan M (2008) Characterization of AC–ZnO catalyst and its photocatalytic activity on 4-acetylphenol degradation. *Catal Commun* 9:262–268
- Sobana N, Krishnakumar B, Swaminathan M (2013) Synergism and effect of operational parameters on solar photocatalytic degradation of an azo dye (Direct Yellow 4) using. *Mater Sci Semicond Process* 16:1046–1051
- Štastná M, Trávníček M, Šlais K (2005) New azo dyes as colored isoelectric point markers for isoelectric focusing in acidic pH region. *Electrophoresis* 26:53–59
- Sun X, Zhang H, Xu J et al (2004) Shape controllable synthesis of ZnO nanorod arrays via vapor phase growth. *Solid State Commun* 129:803–807
- Tsui LS, Roy WR, Cole MA (2003) Removal of dissolved textile dyes from wastewater by a compost sorbent. *Color Technol* 119:14–18
- Umar A, Hahn YB (2006) ZnO nanosheet networks and hexagonal nanodiscs grown on silicon substrate: growth mechanism and structural and optical properties. *Nanotechnology* 17:2174
- Vayssieres L (2003) Growth of arrayed nanorods and nanowires of ZnO from aqueous solutions. *Adv Mater* 15:464–466
- Wu J, Eiteman MA, Law SE (1998) Evaluation of membrane filtration and ozonation processes for treatment of reactive-dye wastewater. *J Environ Eng* 124:272–277
- Yuliarto B, Nulhakim L, Ramadhani MF et al (2015) Improved performances of ethanol sensor fabricated on Al-doped ZnO nanosheet thin films. *IEEE Sens J* 15:4114–4120
- Zhang H, Ma X, Xu J et al (2003) Arrays of ZnO nanowires fabricated by a simple chemical solution route. *Nanotechnology* 14:423

Publisher's Note Springer Nature remains neutral with regard to jurisdictional claims in published maps and institutional affiliations